MET O 19 BRANCH MEMORANDUM NO 33

A Preliminary Analysis of Stratospheric Energetics for 1975/76 Based on Machineable Data

B F Taylor

November 1976

1. Introduction

There are two principal methods of performing diagnostic studies of large-scale atmospheric behaviour: one is the synoptic approach in which a series of selected charts is presented and described in terms of the behaviour of synoptic features, the other is the dynamical approach in which the various forms of atmospheric energy and their interactions are calculated. Although the two methods are not mutually exclusive they do tend to result from different forms of data; a series of hand-drawn charts can reasonably support only the synoptic approach (unless a vast amount of repetitive calculation is to be undertaken) whereas analyses in machineable form can easily be processed to yield the data necessary for the dynamical approach.

While the synoptic approach tends to be somewhat qualitative it has the advantage that it uses the common language of all meteorologists. The dynamical approach has the advantage that, by quantifying some aspect of the energetics, the time variation of the relevant variable may be displayed, often removing the need to present a series of charts for the same purpose.

Perhaps the most fruitful approach is to use the dynamical method to pin-point significant aspects of variations in the circulation and then to describe these in synoptic terms wherever possible.

The stratospheric analysis group is now producing data bases capable of supporting either approach in that:

1) high quality hand-drawn charts at stratospheric levels have been produced daily since April 1974 (Watson 1976),

2) stratospheric charts of similar quality but in machineable form are now being archived (beginning October 1975).

It is hoped that the use of such data will lead, eventually, to the achievement of three main objectives, as follows:

1) a better understanding of both the quiet and disturbed behaviour of the stratosphere and, in particular, of its interaction with the troposphere,

2) the isolation of important or significant features of stratospheric or tropospheric behaviour prior to stratospheric warmings which may lead to the ability to forecast such warmings.

3) the provision of accurate machineable data in a form which can be used by Met O 20 in order to compare the energetics of their numerical model with those of the real atmosphere.

2. Machineable Data

Troposphere

Stratospheric dynamics cannot be studied in isolation but must include the troposphere as an important energy source. Consequently the availability of tropospheric data must be considered.

A Met O 2 objective analysis scheme for levels from the surface to 100 mb has been in operation since 1971. These analyses are used by CFO as the basis of computer forecasts and, as such, are subject to daily monitoring and human intervention aimed at maintaining their accuracy (Singleton 1975). After their use in forecasting they are archived in a form especially convenient for the recreation of direct-access data sets (the so-called print disks) from which analyses, not only of geopotential height but also of temperature and wind information can easily be obtained. Unfortunately, however, as a large amount of further information relating to the forecast, as well as to the analysis, is also archived, retention of the data for long periods is impossible (at present the retention period is eighteen months).

Thus, machineable data up to 100 mb, produced by Met O 2 is easily accessible to Met O 19 (with some reservations about the limited retention period) and may be used by this branch as required.

Stratosphere

A corresponding stratospheric analysis scheme of eight levels from 200 mb to 10 mb has also been running for some years but, because the results were not used in the forecast, no human intervention was applied and, in the data-sparse stratosphere, the analyses were very poor (although much improved with the change from quadric to polynomial fitting in November 1975). Nevertheless these data were (and continue

to be) archived along with the tropospheric analyses on the print disk data sets.

In October 1975 the stratospheric analysis group started to archive analyses in machineable form, based on the Met O 2 objective analyses modified to bring the results into close agreement with the hand-drawn analyses. The modification takes place in two stages, the first of which is similar to the tropospheric intervention of Met O 2 in that the background field for an imminent analysis is modified. Unlike the tropospheric case however, the stratospheric intervention must take place before the hand-drawn charts have been prepared and can be only tentative; nevertheless the more obvious errors are removed and prevent the gradual build-up of gross errors in subsequent analyses; thus reducing the amount of work involved in the final modification of analyses before they are committed to the Met O 19 archive.

The effect of this early intervention is also to improve the stratospheric analyses on the Met O 2 archive. The advantage of this effect is seen when it is realised that the final modification is a very slow process and involves problems of computer availability which have not at the time of writing been completely solved. These problems have resulted in the accumulation of data in the Met O 19 archives being rather slow, with consequent difficulties with regard to an early study of the 1975/76 winter.

In view of this it was decided to use the Met O 2 (Printdisk) data to provide a preliminary view of the dynamical behaviour of the stratosphere during the recent winter. As outlined above, such data contains the benefits of the early intervention but not of the final modification. Any conclusions drawn must therefore be tentative but should indicate the most profitable aspects for investigations when the good-quality data becomes available.

3. Background to the Diagnostic Calculations

The two forms of atmospheric energy considered are kinetic (K) and available potential (A). The concept of available potential energy (developed by Lorenz, 1955) deserves some comment. As demonstrated by Lorenz the use of total potential energy is not helpful in atmospheric studies because potential energy is only available for conversion to kinetic energy when horizontal density gradients occur; these

result in the generation of kinetic energy as the atmosphere adapts itself in such a way as to redistribute mass such that the stratification of density becomes horizontal and statically stable. Lorenz further showed that, by making some approximations, the available potential energy may be expressed in terms of the variance of temperature on an isobaric surface (and the static stability at that surface).

Thus: Available potential energy per unit area averaged over the atmosphere is given by

$$\overline{A} = \frac{1}{2} \int_0^{\overline{p_0}} \frac{1}{\Gamma_d - \overline{\Gamma}} \cdot \frac{\overline{T'^2}}{\overline{T}} \, dp \qquad (1)$$

where a bar denotes a mean over the entire area considered (the whole globe in the case of Lorenz) on an isobaric surface. A prime denotes a deviation from such a mean.

Γ is the temperature lapse-rate

Γ_d is the dry adiabatic lapse-rate

p_0 is surface pressure.

The corresponding expression for kinetic energy per unit area is

$$\overline{K} = \frac{1}{2g} \int_0^{\overline{p_0}} \overline{u^2 + v^2} \, dp \qquad (2)$$

where u and v are the components of velocity.

Although, strictly speaking, these equations apply only to a fixed mass of atmosphere, contained entirely within a fixed region, and as such may only strictly be applied to the whole atmosphere (as envisaged by Lorenz), diagnostic studies have always been confined to restricted regions and between specified pressure levels. (eg the cap north of 20°N from 100 to 10 mb). Smith (1969) points out that such calculations must be interpreted as representing the contribution by a specific region to the available potential energy of the whole atmosphere rather than as the available potential energy of the region itself.

A common practice used in the study of the global circulation is to resolve each of the two forms of energy into zonally-meaned and eddy components and this practice is followed here.

Rather than integrating over a range of pressure and presenting energy values for that layer, the integrands themselves were calculated at individual pressure levels, thus producing values of energy per unit area per unit pressure; unit pressure in the SI system being 1 Nm^{-2}. Multiplication by 100 then produced answers in the meteorologically convenient units of $Jm^{-2}mb^{-1}$.

The basic equations now become:

Zonally meaned available potential energy,

$$\overline{A_Z} = \frac{100}{2} \frac{\overline{[T]'^2}}{(\Gamma_d - \overline{\Gamma}).\overline{T}} \qquad (3)$$

Eddy available potential energy,

$$\overline{A_E} = \frac{100}{2} \frac{\overline{T^{*2}}}{(\Gamma_d - \overline{\Gamma}).\overline{T}} \qquad (4)$$

Zonally meaned kinetic energy,

$$\overline{K_Z} = \frac{100}{2g} \overline{[u]^2 + [v]^2} \qquad (5)$$

Eddy kinetic energy,

$$\overline{K_E} = \frac{100}{2g} . \overline{u^{*2} + v^{*2}} \qquad (6)$$

where $[\,(\,)\,] = \frac{1}{2\pi} \int_0^{2\pi} (\,)\, d\lambda$ or "zonal mean" (λ being longitude)

$\overline{(\,)} = \frac{1}{\sin\phi_2 - \sin\phi_1} \int_{\phi_1}^{\phi_2} [(\,)] \cos\phi \, d\phi$ or "overall mean"

N.B. Whereas Lorenz averaged over the entire globe the region of study here was from latitude $\phi_1 = 19^\circ N$ to latitude $\phi_2 = 89^\circ N$.

$(\,)^* = (\,) - [(\,)]$ or the deviation from a zonal mean

$(\,)' = (\,) - \overline{(\,)}$ or the deviation from the overall mean.

Variations on this notation are used in the literature but this form is probably the simplest. From these definitions it follows that $[T]'$ denotes the deviation of a zonally-meaned temperature from the overall mean, hence it may be seen that $\overline{A_Z}$ reflects the variance associated with the meridional temperature gradient while $\overline{A_E}$ reflects the temperature variation around a latitude circle.

A further common technique also adopted in this study is to resolve $\overline{A_E}$ and $\overline{K_E}$ into the various wave numbers. This may be done simply by applying versions of equations 4 and 6 in which the total variances $\overline{u^{*2}}$, $\overline{v^{*2}}$ and $\overline{T^{*2}}$ are replaced by the variances in the approriate wave number.

$\hat{u}^2(n)/2$, $\hat{v}^2(n)/2$ and $\hat{T}^2(n)/2$ where $\hat{u}(n)$, $\hat{v}(n)$ and $\hat{T}(n)$ are the amplitudes of the u, v and T waves in wave number (WN) n around a latitude circle.

Thus
$$\overline{A_E(n)} = \frac{100}{4} \frac{\overline{\hat{T}^2(n)}}{(\Gamma_d - \bar{\Gamma}).\bar{T}} \tag{7}$$

$$\overline{K_E(n)} = \frac{100}{4g} \overline{(\hat{u}^2(n) + \hat{v}^2(n))} \tag{8}$$

The rate of change of K_E in a layer, neglecting horizontal transfers across the vertical boundary at the edge of the layer is given by:-

$$\frac{\partial \overline{K_E}}{\partial t} = -\frac{\partial}{\partial p}(\overline{\omega K_E}) - 100 \frac{\partial}{\partial p}(\overline{\omega^* z^*}) + CE + CK - DE \tag{9}$$

where $\omega = Dp/Dt$, the vertical velocity in pressure co-ordinates,

CE and CK are conversions to $\overline{K_E}$ from $\overline{A_E}$ and $\overline{K_Z}$ respectively and DE is the dissipation rate of $\overline{K_E}$.

The presence of the factor of 100 follows from the definition of $\overline{K_E}$ in eqn 6.

Both of the first two terms on the R.H.S. of eqn 9 act to transfer $\overline{K_E}$ from one level to another; the first one directly, the second via the flux of geopotential. This second term has been found to be the dominant term of the two and to control energy exchanges in the vertical (Muench 1965 , Miller and Johnson 1970).

Although no attempt is made here to perform a complete budgetary analysis, this term, known as the "pressure-interaction" term and the "flux of geopotential" (F.O.G.) was evaluated at various stratospheric levels. In order to avoid calculating W, Miller and Johnson resorted to the approximation of Eliassen and Palm (1960) which relates $\overline{W^*Z^*}$ to the northward eddy heat flux:-

$$\overline{\omega^* z^*} \simeq \frac{f}{g}\left(\frac{\partial [\theta]}{\partial p}\right)^{-1} [u]\,\overline{[v^* \theta^*]} \tag{10}$$

or in terms of individual wave numbers

$$\overline{\omega^* z^*(n)} \simeq \frac{f}{g}\left(\frac{\partial[\theta]}{\partial p}\right)^{-1}[u]\,\overline{\frac{\hat{v}(n)\,\hat{\theta}(n)}{2}\cos(\Delta\phi(n))} \qquad (11)$$

where θ is potential temperature and $\Delta\phi(n)$ is the phase difference between the waves of v and θ in WN.n.

4. Procedure

00 GMT. Octagon analyses at two-day intervals from the beginning of November 1975 until the end of March 1976 were accessed (either while the data were current or by subsequent recreation of the data sets from archival tape). Because the octagon grid is rectangular (on a polar stereographic projection) while equations 3 through 11 involve zonal means it was necessary to transfer the data onto a grid with points set on longitude circles. The "High Resolution Grid" of Met O 20 was chosen and an interpolation routine supplied by that branch was modified for the purpose of converting the data on to grid points set on latitude circles at two-degree intervals from 19°N to 89°N. After interpolation the data was processed to yield values of $\overline{A_Z}$, $\overline{A_E}$, $\overline{K_Z}$ and $\overline{K_E}$ at six levels, viz 1000, 500, 300, 100, 50 and 20 mb. Kinetic energy calculations alone were performed also at 10 mb; temperatures are not calculated operationally at this level because there is no height analysis above 10 mb and consequently no thickness upon which to base 10 mb temperatures.

Moreover as the print disk data sets do not contain wind data at levels above 100 mb geostrophic winds were calculated at 50, 20 and 10 mb for use in the computations.

Fourier analysis was performed on the wind and temperature field around each of the thirty six available latitude circles to reveal the contributions to $\overline{A_E}$, $\overline{K_E}$ and $\overline{\omega^* z^*}$ made by the first six wave numbers. For programming reasons the total value of $\overline{\omega^* z^*}$ was not calculated as such but was approximated by the sum of the first six wave numbers.

As outlined above the calculations performed on levels up to and including 100 mb may be taken as "final" whereas the results based upon analyses at the three upper levels will be subject to revision when the final (Met O 19) data sets become available.

In addition, the same calculations were performed on archival data for the previous winter (1974/75) at 1000, 500, 300 and 100 mb, also at two-day intervals. During that winter no intervention above 100 mb was attempted and consequently the analyses at these stratospheric levels are not sufficiently accurate even for the purpose of a preliminary study.

5. Results

As a result of archiving problems in Met O 2 there was some loss of stratospheric print disk data in late February and March 1976. ØØ GMT data were lost up to the end of the period of interest but 12 GMT data were lost only up to 8 March, consequently the following time sections show 12 GMT data from 9 March. While this is to be regretted in view of the fact that the final warming occurred during this period, the loss applies only to print-disk data and subsequent diagnostic calculations may still be made when the final Met O 19 data set becomes available.

Time sections showing the variation of various aspects of the atmosphere up to 10 mb are presented.

5.1 Eddy Kinetic Energy

Fig 1 shows eddy kinetic energy in the first two wave numbers. The variations show a remarkable continuity in the vertical, with peaks at 10 mb often being traceable down to 500 mb. Where this occurs there is a near simultaneity in the vertical which is in conflict with the findings of Muench (1965) who observed a five or six day lag between a wave's reaching its maximum amplitude at 500 mb and its doing so at 10 mb.

Quiroz and Nagatani (1976) who have performed a similar analysis on this winter presented a diagram very similar to that in fig 1 based on NMC analyses for 10°N to 90°N (cf 19°N to 89°N here) except that height amplitudes

are plotted instead of kinetic energies - agreement is sufficient to be reassuring. They made the point that the WN.1 oscillation peaking at the very end of November at 10 mb appears to lay downwards to 4 December at 500 mb (65°N) and 6 December (45°N). The timing indicated by fig 1 is slightly different but the lag appears in the same sense, from 2 Dec at 10 mb to 8 Dec at 500 mb. However, much of the change in fig 1 appears between 50 and 100 mb at the transition from the stratospheric analysis scheme to the tropospheric version, whereas Quiroz and Nagatani showed the lag as appearing more gradually and suggest that this is an example of "stratospheric feedback".

The clear continuity down to 500 mb is not always present, eg the 10 mb WN1 peaks of early February and mid March and the WN2 peak of late January. Moreover, the presence of strong peaks at 500 mb does not in itself guarantee their presence at 10 mb.

From the timing of the 'Stratalert - warming in progress' messages issued by the Free University of Berlin it may be seen that these coincided with significant changes in the 10 mb circulation, from WN1 to WN2 in early January and from WN2 to WN1 and back to 2 in early February. Although the data for the beginning of the final warming are missing, inspection of the calcomp charts produced while the data were still current, indicates that the period was marked by a decline in WN1 and an increase in WN2 (as may be seen also at 100 mb). Furthermore, Quiroz and Nagatani have pointed out an early winter warming in mid to late November which was confined to the lower and middle stratosphere. Stratalert messages are not issued before 1 December and in any case the rate of warming was very close to (and probably just below) the limit necessary for the issuing of a warning. Nevertheless the period was marked by a significant peak in WN2, associated with a temporary decline in WN1. Thus the onset of all four warmings during this winter were associated with the decline of eddy kinetic energy in one wave number and its increase in another. It may be significant that the rise of kinetic energy in WN1 from mid to late December at 10 mb was not itself associated with a warming but the warming commenced after the WN1 peak with the rise of WN2 energy.

Fig 1 may also be inspected from the point of view of the objective, stated in the introduction, of determining some feature of the tropospheric or stratospheric circulation preceding the warming events.

In a numerical modelling experiment which successfully produced a warming, Matsuno (1971) initially assumed that "In the troposphere planetary scale disturbances (zonal wave numbers 1, 2) grow with time to reach an unusually large amplitude and persist for a long time". Matsuno's forcing wave at 10 km was "switched on" at day 0 and rose to its peak (and subsequently constant) value around day 5. For the WN2 case a warming rate consistent with the issuing of a stratalert warming in a real case was achieved by about day 20 (at which time the wave amplitude at 10 mb had just reached its peak). This delay of (say) 15 days was increased by a few days when either the forcing wave was switched off around day 20 or a forcing wave of lower amplitude was used. Both of these changes also reduced the observed temperature rise. However, Matsumo was unable to determine a threshold forcing amplitude, below which no stratospheric warming was produced, nor did he describe any experiment to determine a threshold forcing duration.

Following this work it would seem reasonable to seek a rise of eddy kinetic energy in some wave number at 300 mb to an "unusually large" value which persists at this value for something over two weeks. It may then be hoped to associate this with a stratalert period some two to three weeks after the initial rise of 300 mb eddy kinetic energy.

Unfortunately, for various reasons this approach to the forecasting problem does not seem helpful. The two mid-winter stratalert periods were associated with only very minor warmings and, in view of Matsuno's failure to fix threshold conditions for successful forcing it remains possible that relatively minor and transient forcing would have caused them. The delay of two or three weeks ascertained by Matsuno is comparable with the intervals between stratalert periods of the 1975/76 winter and this would make the unambiguous allocation of a forcing source to each period very difficult. But perhaps the main difficulty is caused by the fact that the delay between the rise of the wave

amplitude at 300 mb and the appearance of the peak wave amplitude at 10 mb appears much greater than was the case in the 1963 warning upon which Matsuno's theoretical work was based (Hirota and Sato, 1969) and in view of the above comments about the near simultaneity of all levels (and the corresponding comments of Quiroz and Nagatani, 1976) it is hard to imagine the 300 mb behaviour providing useful forecasting information for the stratosphere some two weeks or more ahead.

5.2 Zonally meaned and Eddy Kinetic energy

Fig 2 shows the variation of $\overline{K_Z}$ and $\overline{K_E}$. The principal characteristics expected of stratospheric warmings, so far as kinetic energy is concerned, are a decline in $\overline{K_Z}$ and a rise in $\overline{K_E}$ during the early part of the warming (as the zonal flow breaks down and is replaced by eddies). The subsequent behaviour of these two variables depends on the strength of the warming and, where the warming is minor, a rapid return by $\overline{K_E}$ and $\overline{K_Z}$ to their approximate pre-warming values is to be expected.

Fig 2 illustrates the fact that in neither of the mid-winter stratalert periods were these characteristics present (at 20 and 10 mb). During the warming of early January $\overline{K_Z}$ actually rose while $\overline{K_E}$ fell and during the warming of early February both forms of kinetic energy decreased. On the other hand, the warming of late November did possess the expected characteristics as did (so far as one can judge by interpolation through the missing data period) the final warming.

The failure of the two mid-winter warmings to have the expected affect on the kinetic energy values results, presumably, from the failure of the warmings to penetrate sufficiently far north and/or to a sufficiently low altitude. No description of comparable warmings has been found in the literature; where a "Minor Warming" has been studied (eg Klinker 1976) it was (unlike the warmings of January and February 1976) sufficiently intense to reverse the mean meridional temperature gradient north of $60^{\circ}N$.

It appears then that the only kinetic energy effects associated with the minor mid-winter warmings are the rapid transitions of eddy kinetic energy between wave numbers one and two described above.

One further aspect of fig 2 is interesting. Only one peak of $\overline{K_E}$ is identifiable at all levels - that of late November. The peak occurs on 22 November at 1000 mb and (within the time resolution of the graph) appears with increasing lag at successive levels, occurring on 28 November at 10 mb. This indicates a vertical propagation speed of disturbance energy of between 5 and 6 km day^{-1}, which is in agreement with the speed given by Muench (1965) for the propagation speed of energy in individual wave numbers. By referring again to fig 1 it may be seen that the peak is dominated by energy in WN2, however the peak in $\overline{K_E}(2)$ alone appears instantaneously at all levels; the lag is only introduced when energy in other wave numbers is included. While the interpretation of this result is unclear, it may indicate that the transfer of energy between different wave numbers is a significant feature of the upward propagation of eddy kinetic energy. Hence it may have a bearing on the paradox presented by the apparently instantaneous propagation of wave energy through the atmosphere gained from graphs such as fig 1.

5.3 Eddy available potential energy

Fig 3 shows the time variation of $\overline{A_E}$ by wave number. Temperatures are calculated from thicknesses and hence are particularly sensitive to errors in height analysis. In particular, it has been found that the 50 and 20 mb temperatures on certain days investigated were particularly inaccurate and this fact must be borne in mind during consideration of the following discussion.

Fig 3 may be related to fig 1 in the following rough and ready manner. $\overline{A_E}$ is associated with temperature waves around latitude circles (eqns 4 and 7) and eddy kinetic energy is associated with geopotential height waves in the same direction (Johnson et al 1969) although this latter association is very rough. Clearly, from the hydrostatic equation, geopotential height waves in a particular wave number at a given pressure level must be associated with

temperature waves in the same wave number at some lower level. Phase considerations are also important in that eg WN1 temperature fields at 500 and 300 mb which have phases differing by 180° will tend to cancel, leading to there being a lower geopotential variance in WN1 at say 100 mb than at 300 mb. Nevertheless fig 3 and fig 1 may conveniently be related by assuming (a) that such cancellations are not usually significant and (b) that the correlation between geopotential wave amplitude and kinetic energy in the corresponding wave number is significant.

Thus the high values of kinetic energy in WN1 which persist from 8 Nov to 16 Nov at 100 mb and from 10 Nov to 20 Nov at 10 mb are related to WN1 temperature peaks in the troposphere on 8th and 16th superimposed on a WN1 temperature field at 50 mb peaking on 10th and 24th (8th and 22nd at 20 mb)- this kinetic energy wave, at least, does appear to lag in the sense shown by Muench. The next kinetic energy peak in WN1 (2 Dec at 10 mb) referred to earlier has its origin, at the upper levels, in association with temperature waves peaking on 2 Dec at 50 mb and 4 Dec at 20 mb while its appearance at tropospheric levels is associated with strong temperature wave peaks at 1000 and 500 mb on 6 Dec. In both of the above examples the $\overline{A_E}(1)$ curve is relatively flat indicating some independence between the temperature waves of troposphere and stratosphere, while the corresponding wave in the flow field is apparently continuous.

One other aspect of fig 3 is interesting; all three stratalert periods were immediately preceded by $\overline{A_E}(1)$ peaks at 100 mb. The early warming (November) which is not marked by a stratalert period is an exception but this warming was (as described above) unusual in being confined to the lower and middle stratosphere, moreover a strong WN1 peak at 300 mb did occur on 16 November.

The connection between the behaviour of the 100 mb available potential energy in WN1 and the occurrence of the stratalert periods is made clearer when an extended vertical scale is used (Fig 4). It may be seen also that a similar correspondence was present during the winter of 1974/75 (with the

exception of a very short-lived Stratalert period in mid December).

The question naturally arises as to whether this feature could be a useful indicator of imminent warming events; but the question may only be answered by observing future winters to determine whether the correlation persists or by determining some causal connection between the two phenomena. One possible explanation is related to the behaviour of the $\overline{W^* Z^*}(1)$ term.

5.4 The Pressure Interaction Term (or Flux of Geopotential) Relationship to the 100 mb Temperature Structure

From eqn 11 it follows that the magnitude of $\overline{W^* Z^*}(n)$ is proportional to $\hat{\theta}(n)$. An increase in the amplitude of the temperature wave will lead to an increase in the magnitude of the $\overline{W^* Z^*}$ term in the corresponding wave number unless other variables on the R.H.S. of eqn 11 change to counteract this. But $\overline{A_E}(n)$ is also controlled by the same factor (eqn 7). Thus, a peak in $\overline{A_E}(1)$ is likely (but not certain) to be related to a peak in $\overline{W^* Z^*}(1)$ and hence to be associated with the transfer of $\overline{K_E}(1)$ upwards through the 100 mb level. As the 10 mb value of $\overline{K_E}(1)$ undergoes significant changes during all the warmings investigated it seems plausible that the 100 mb $\overline{A_E}(1)$ peaks and the onset of the warmings are related through the pressure interaction term. It is emphasized that the $\overline{A_E}(1)$ peaks are interpreted here as being indicators of large amplitude temperature waves in WN1 - no dynamic connection between 10 mb $\overline{K_E}(1)$ and 100 mb $\overline{A_E}(1)$ as such is suggested.

To test this hypothesis the time variations of $\overline{W^* Z^*}(1)$ at 100 mb for both winters were plotted (fig 5). A three-point running mean was used in order to reduce the considerable noise-level present. By comparing figs 4 and 5 it may be seen that the peaks in $\overline{A_E}(1)$ preceding five of the six stratalert periods correspond to $\overline{W^* Z^*}(1)$ peaks occurring at roughly the same time. Correspondence in time is very close indeed except in the case of the $\overline{W^* Z^*}(1)$ peak of late December 1974 which lags the "corresponding" $\overline{A_E}(1)$ peak by six days (presumably as a result of the behaviour of other factors on the R.H.S. of eqn 11). The correlation between the two quantities 100 mb $\overline{W^* Z^*}(1)$ and 100 mb $\overline{A_E}(1)$ (also subjected to a three-point running mean smoothing for the sake of

consistency) over the period of main interest from 10 December to 10 March was −0.57 for 1974/75 and −0.67 for 1975/76; these values are significant at the 0.1% probability level. Over the entire periods shown in fig 5 the correlations were numerically lower but still significant at the 0.1% level.

It is possible to associate the 100 mb $\overline{W^{*} Z^{*}}(1)$ peaks of late December 1975 and late February 1976 with the increases of 10 mb $\overline{K_E}(1)$ which occurred before the first and last stratalert periods of that winter (the warmings actually began as $\overline{K_E}(1)$ declined). On the other hand, the 100 mb $\overline{W^{*} Z^{*}}(1)$ peak of 1 February 1976 must be associated with the rise of $\overline{K_E}(1)$ at 10 mb during the early part of the second stratalert period. This interpretation is consistent with the observation that the $\overline{W^{*} Z^{*}}(1)$ peak associated with the second stratalert period occurred later in relation to that period than did the other two peaks in relation to their corresponding stratalert periods.

Thus, using the above arguments, it is possible to relate the peaks of 100 mb $\overline{A_E}$ (1) (fig 4) to the onset of the warmings via the mechanism of the pressure interaction term. The importance of the latter in connection with warming events is already well known (eg Miller and Johnson, 1970) and will be discussed further in the following section; but the term simply indicates an export of energy from the troposphere and the reasons for sudden increases in this export are not understood in terms of tropospheric behaviour. Perhaps by studying the behaviour of the 100 mb temperature field (as discussed here in terms of $\overline{A_E}(1)$ during future winters those tropospheric conditions which give rise to an increased export of energy to the stratosphere may be identified.

The Controlling Effect on $\overline{K_E}$

The control exerted by the flux of geopotential through 100 mb or the flow above has been demonstrated by Miller (1970) who calculated lag correlations between $(\overline{W^{*} Z^{*}}(2) - \overline{W^{*} Z^{*}}(1))$ at 100 mb and values of an index which is roughly proportional to $(\overline{K_E}(2) - \overline{K_E}(1))$ at 10 mb. The index was used to avoid calculating the kinetic energies themselves. Highly significant correlations were found

at lags between 0 and 6 days (the 10 mb circulation lagging the energy flux).

Comparing figs 1 and 5b it may be seen that the behaviour of 10mb $\overline{K_E}$ does indeed appear to follow the variation of the 100 mb $\overline{W^* Z^*}$ in the corresponding wave number with a lag of several days. Correlations were evaluated in each wave number for various lags after first subjecting the $\overline{K_E}$ values to a three-point running-mean smoothing to make them consistant with the $\overline{W^* Z^*}$ values which had already been so treated. The results, shown in table 1, are consistent with those of Miller but are expressed rather more simply in that the wave numbers are treated separately.

Table 1. Lag correlations between 10 mb $\overline{K_E}(n)$ and 100 mb $\overline{W^* Z^*}$ (n) for n=1 and 2. Positive lag indicates that the 10 mb $\overline{K_E}$ (n) lags the 100 mb $\overline{W^* Z^*}(n)$

Lag (days)	-4	-2	0	2	4	6	8	10	12	14
No of pairs	53	54	55	54	53	52	51	50	49	48
Correlation Coefficient, WN1	0.07	-0.10	-0.29	-0.47	-0.59	-0.62	-0.57	-0.48	-0.35	-0.21
Correlation Coefficient, WN2	-0.12	-0.29	-0.47	-0.65	-0.75	-0.69	-0.57	-0.42	-0.28	-0.15

Correlations significant at the 0.1% probability level occur for lags of 2 to 10 days for WN1 and 0 to 8 days for WN2, slightly longer than the 0 to 6 days given by Miller.

Although the flux of geopotential through 100 mb is only one of several factors influencing the behaviour of $\overline{K_E}$ at the higher levels, its controlling influence is clearly demonstrated by the above results.

The observed lag may also be interpreted in the following way. Referring again to fig. 5b, the WN1 flux which is always negative (upwards) may be separated into a steady component of -100 mW m^{-2} and a variable component which is very roughly sinusoidal with amplitude 100 mW m^{-2} and period about 30 days. Now, in view of the correlations presented above for 10 mb and the similarity of the 50 and 20 mb $\overline{K_E}(1)$ to that at 10 mb, the varying component may be identified with variations of $\overline{K_E}(1)$ at levels within the 100 mb - 0 mb region and the steady component with an equal, steady leakage from $\overline{K_E}(1)$ into some other form of energy.

Some such leakage must be present or else a continuous upward flux would produce a continuous rise in $\overline{K_E}(1)$ which is not observed at any level, even at those above 10 mb not shown here.

The upward flux in WN1 at 100 mb is now defined by:-

$$F(1) = \hat{F} \sin(ft) \qquad \text{where } f = 2\pi/T$$

and T is the period

Assuming that all the flux through 100 mb converges continuously in the layer 100 mb - 0 mb, tending to 0 as p tends to 0 then the mean value of $\overline{K_E}(1)$ for this layer ($\widetilde{K_E}(1)$) is given by:-

$$\frac{\partial \widetilde{K_E}(1)}{\partial t} = \frac{F(1)}{\Delta p} \qquad \text{where } \Delta p = 100\,mb$$

Initial conditions of $\widetilde{K_E}(1) = 0$ at $t = 0$ then yields the solution:-

$$\widetilde{K_E}(1) = \frac{\hat{F}}{f\Delta p}\left\{1 + \sin(ft - \pi/2)\right\}$$

Thus $\widetilde{K_E}(1)$ varies sinusoidally about a mean value of $\hat{F}/f\Delta p$, with an amplitude of $\hat{F}/f\Delta p$, a period equal to that of the forcing and lags the forcing wave by $\pi/2$. The lag is thus 30/4 days or about 7 days which is consistent with the results of the lag correlation tests. $\hat{F}/f\Delta p$ is about 400 J m^{-2} mb^{-1} but this cannot be checked against observation (fig.1) because a significant flux passes upwards through 10 mb (hence the contribution of the 10 to 0 mb region to $\widetilde{K_E}$ is also significant).

The effect of a finite propagation speed of this energy has not been included; rather it has been assumed that the energy is communicated instantaneously to all levels. The additional delay introduced by a propagation speed of about 6 km day^{-1} between 100 and 10 mb would be 2 to 3 days.

Convergence of the Term

Klinker (1976) points out the fact that there is no limiting value of the pressure interaction term which, when exceeded, allows the forecasting of a major warming event. In any case the build-up of eddy kinetic energy within a layer depends upon the flux divergence for that layer (eqn. 9); consequently the study of this divergence may lead to the development of some indicator of an imminent warming

whereas the value of the flux itself has failed to do so.

Fig. 6 shows the time variation of energy convergence through the eddy pressure interaction term for wave numbers 1 and 2 within the 50 to 20 mb layer (ie 20 mb $\overline{W^* Z^*}(n)$ -50 mb $\overline{W^* Z^*}(n)$). The convergences presented here were smoothed by means of a 3-point running mean. No corresponding section of kinetic energy, meaned over the same layer, has been produced but the individual 50 and 20 mb sections (fig. 1) are sufficiently similar in shape to suffice for the purpose of comparison with fig. 6.

Some aspects of the two figures are reasonably consistent eg the rise of kinetic energy in WN2, (50 mb) turning to a decrease around 16 February and the energy convergence in that wave number becoming negative around the same time. The consistency is not maintained throughout however, eg the rise in $\overline{K_E}(2)$ continuing up to about 23 January while the energy convergence becomes negative on the 16 January. The disagreements, where they occur, may be a reflection either of the importance of other terms in the kinetic energy budget or of shortcomings in the temperature data, referred to earlier, and used in the computation of $\overline{W^* Z^*}$.

The principal reason for presenting fig. 6 is the similarity which it bears to a corresponding diagram shown by Klinker for the convergence of the term in the 50 to 10 mb layer during warming events of 1970/71 and 1974/75. Klinker points out that the layer exports eddy kinetic energy into the upper stratosphere during the week prior to the reversal of the temperature gradient, thus being a major energy source for high level warming. The downward propagation of the warming eventually limits the vertical eddy flux through 10 mb and leads to a strong convergence within the 50 to 10 mb layer which produces the build-up of eddy kinetic energy characteristic of the breakdown. Thus the strong divergence of the eddy pressure interaction term followed by a strong convergence is suggested as a characteristic of warming events.

In the warming of early February 1976 (fig. 6) the convergence pattern clearly possesses this characteristic pattern. The partitioning by wave numbers further shows that in this case the pattern exists in wave numbers 1 and 2. Wave number 2 is dominant and leads WN1 by several days. At the time of the data loss it

appears that WN2 is in the process of repeating the cycle as the final warming takes place.

On the other hand the early January warming, failed to produce any such pattern. Study of the charts and Berlin's stratelert commentary indicates that downward penetration of this warming below 10 mb was very limited (as compared with the early February event) and it may be that this limited downward penetration prevented the appearance of the characteristic configuration in the 50 to 20 mb convergence pattern.

Two points remain unclear; the continued build-up of kinetic energy in WN2 even after the eddy flux becomes divergent in mid-January must be investigated further when the more reliable data becomes available. Secondly, the limiting of the upward eddy flux through 10 mb by the downward propagation of the warming (Klinker) is not entirely explained by the reversal of the temperature gradient in the absence of a zonal wind reversal. Reed et al (1963) have shown that the eddy heat flux may continue in a northward direction even against the temperature gradient and from eqn. 10 such conditions will maintain $\overline{W^* Z^*}$ in the upward sense.

6. Concluding Remarks

It has been seen that the availability of machineable data produced by Met O 2b renders detailed, real-time monitoring of atmospheric behaviour fairly easy.

It is planned to perform the same computations on current data throughout the coming winter (1976/77) and to increase the amount of intervention in the stratospheric objective analysis. This should make more reliable the results of the calculations performed on the stratospheric data.

The exact nature of the treatment of the high-quality stratospheric data being archived by Met O 19 is, as yet, undecided. Work is in hand to modify these data into a form suitable for their use with the diagnostic programs developed by Met O 20 and experiments will shortly begin to determine whether the data possesses sufficient internal consistency and smoothness to be an acceptable alternative to model-generated data. Should the experiments reveal the data and the Met O 20

diagnostic programs to be incompatible then the programs used in the present study will be modified for application to the final data. Otherwise the full diagnostic programs will be used to calculate not only the day to day variations of the various forms of energy but also the transformations between energy forms, including non-linear interactions between different wave numbers.

References

ELIASSEN, A and PALM, E. 1960 On the transfer of energy in stationary mountain waves. Geofys. Publ., 22, pp. 1-23.

HIROTA, I and SATO, Y. 1969 Periodic variation of the winter stratospheric circulation and intermittent vertical propagation of planetary waves. J.Met.Soc.Japan, 47 pp. 390-402.

JOHNSON, K.W., MILLER, A.J. and GELMAN, M.E. 1969 Proposed indices characterizing stratospheric circulation and temperature fields. Mon.Weather Rev., 97, pp.565-570.

KLINKER, E. 1976 The energetics of the stratosphere during the warming period 1974/75. Presented at XIX COSPAR meeting, Philadelphia, U.S.A.

LORENZ, E. 1955 Available potential energy and the maintenance of the general circulation. Tellus, 7, p. 157-167.

MATSUNO, T. 1971 A dynamical model of the stratospheric sudden warming. J. Atmos. Sc., 28, pp. 1479–1494.

MILLER, A.J. 1970 The transfer of kinetic energy from the troposphere to the stratosphere. Ibid., 27, pp. 388–393.

MILLER, A.J. and JOHNSON, K.W. 1970 On the interaction between the stratosphere and troposphere during the warming of December 1967 – January 1968. Q.J.R. Met. Soc., 96 pp. 1–13.

MUENCH, H.S. 1965 On the dynamics of the winter time stratosphere circulation. J.Atmos. Sc., 22, pp. 349–360.

QUIROZ, R.S. and NAGATANI, R.M. 1976 A study of tropospheric–stratospheric interaction based on combined satellite and rawinsonde data. Presented at COSPAR Symposium C, XIX COSPAR Meeting, Philadelphia, U.S.A.

REED, R.J., WOLFE, J.L. and NISHIMOTO, H. 1963 A spectral analysis of the energetics of the stratospheric sudden warming of early 1957. Ibid., 20, pp. 256–275.

SINGLETON, F. 1975 Human intervention in the operational objective analysis. Met. Mag., 104, pp. 323–330.

SMITH, P.J. 1969 On the contribution of a limited region to the global energy budget. Tellus, 21, pp. 202–207.

WATSON, N.R. 1976 The 1974/75 stratospheric winter. Met. Mag., 105, pp. 69–86.

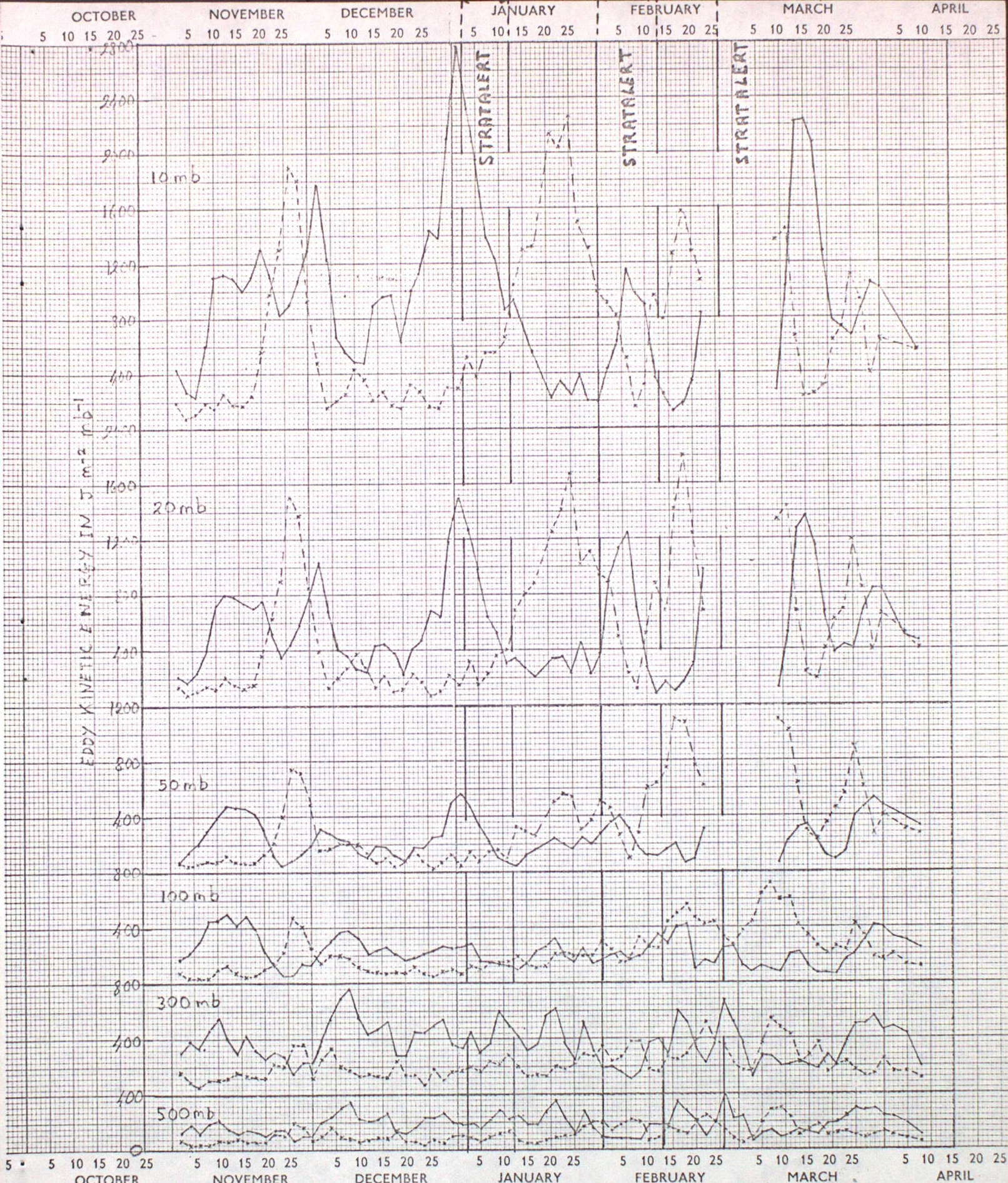

Figure 1. Eddy kinetic energy in wave numbers 1 and 2 for 1975/76. In this and subsequent figures the values are based on 00 GMT data except from 9 March 1976 onwards at 50, 20 and 10 mb where 12 GMT data were used. Periods marked are those during which Berlin's Stratalert messages indicated that warmings were in progress.

——— $\overline{K_E(1)}$

x- - - - x $\overline{K_E(2)}$

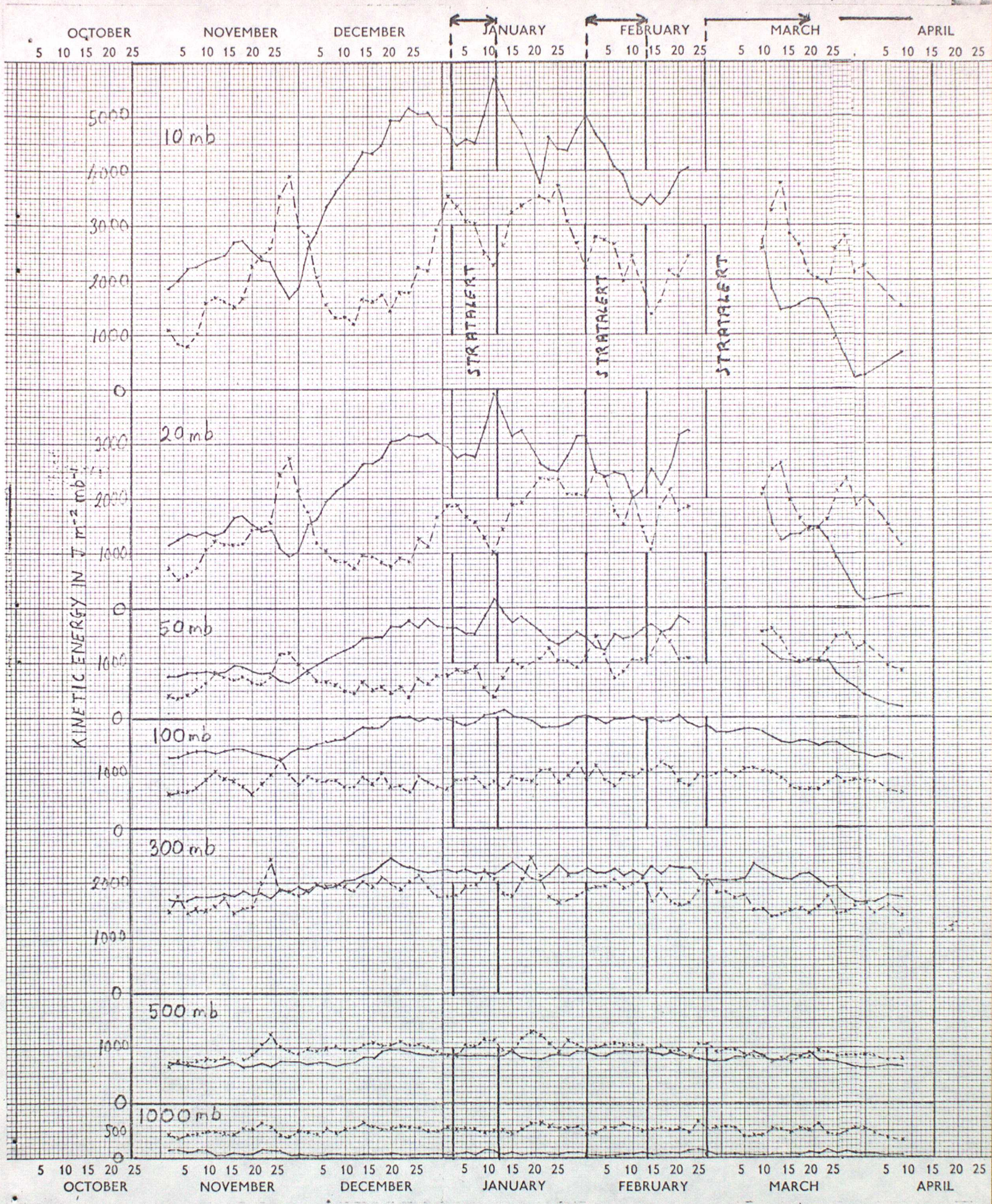

Figure 2. Zonally-meaned and eddy kinetic energy for 1975/76

$\overline{K_Z}$

x- - - -x $\overline{K_E}$

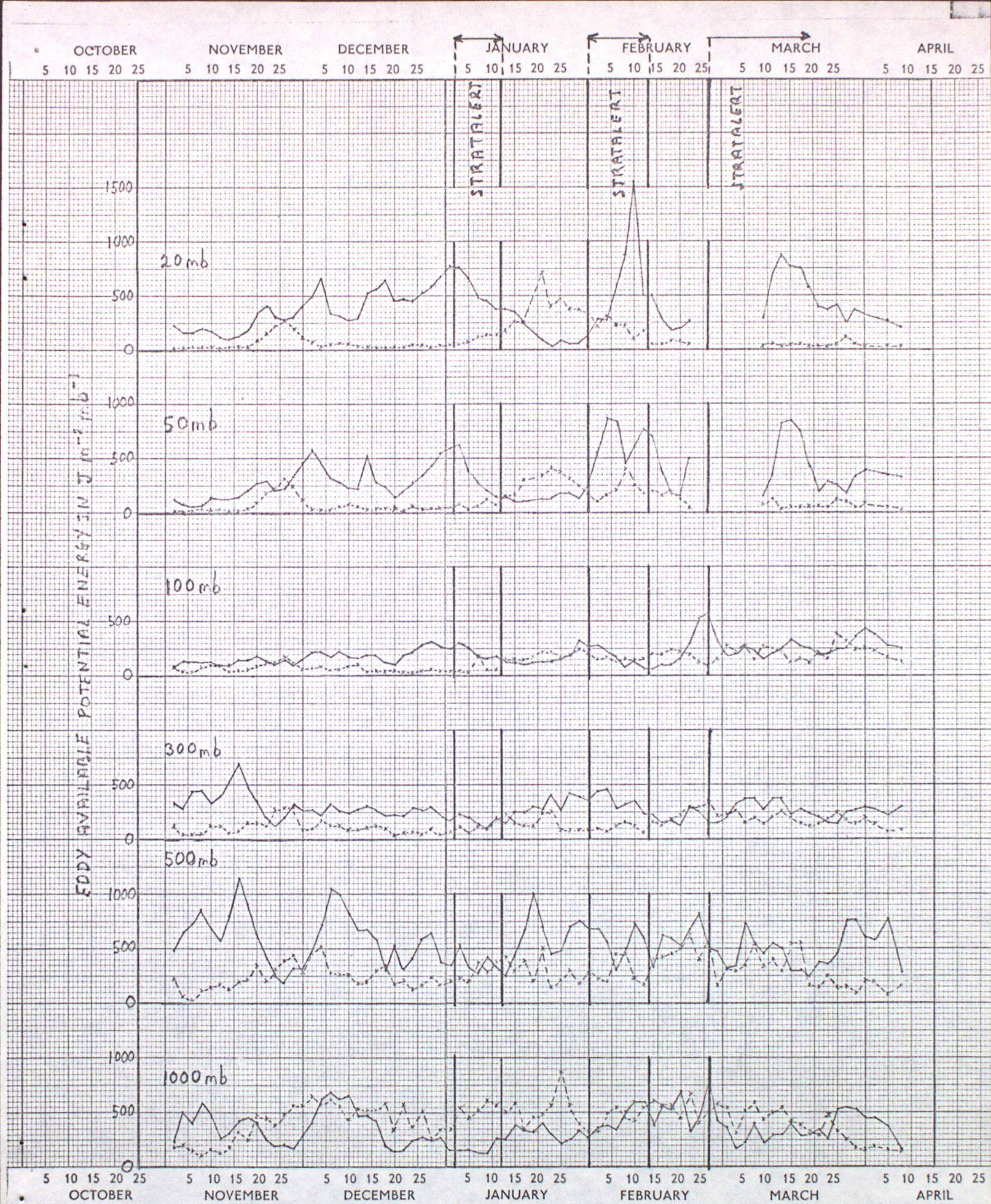

Figure 3. Eddy available potential energy in wave numbers 1 and 2 for 1975/76.

———— $\overline{A_E}(1)$

x- - - - -x $\overline{A_E}(2)$

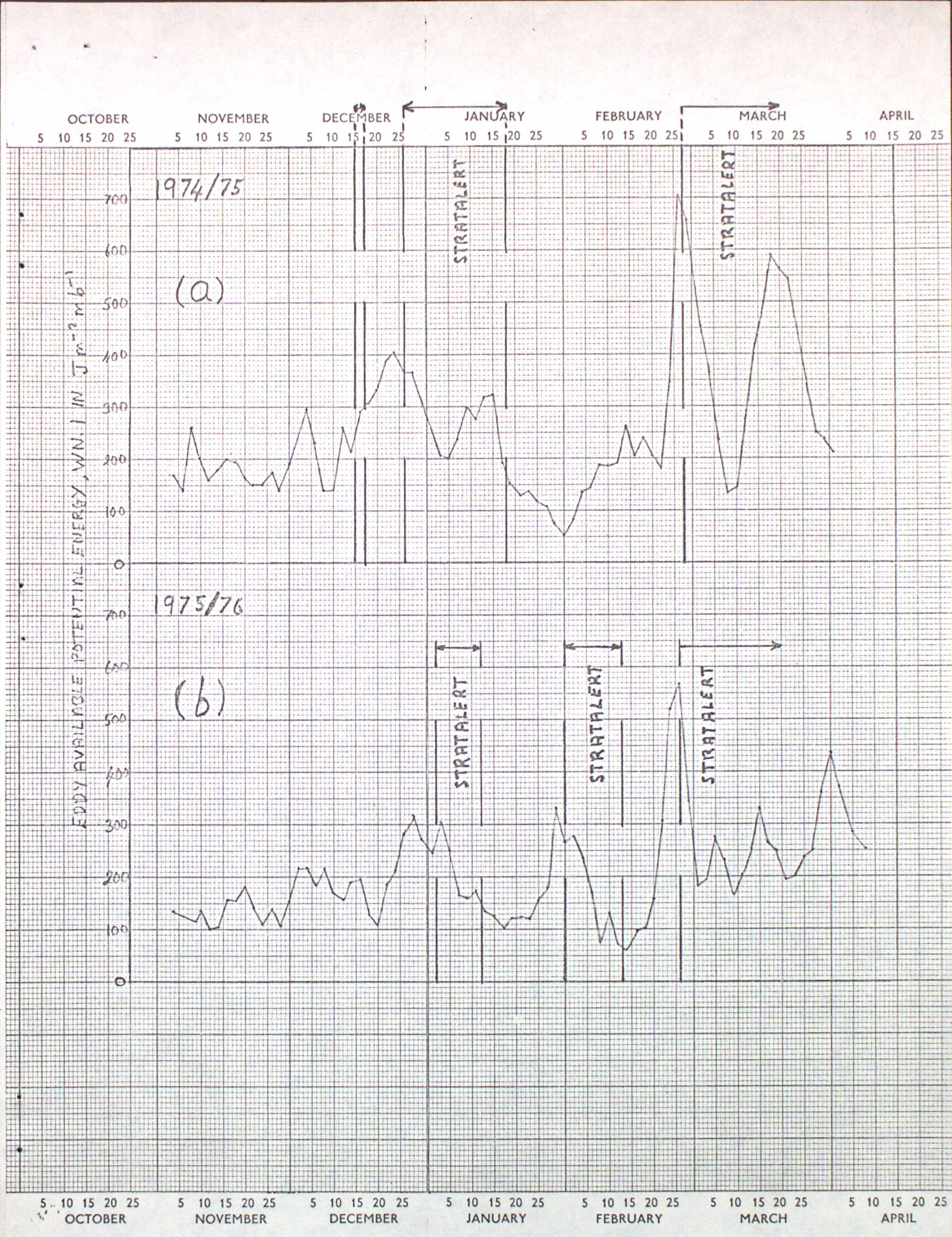

Figure 4. 100 mb eddy available potential energy in wave number 1 for two winters.

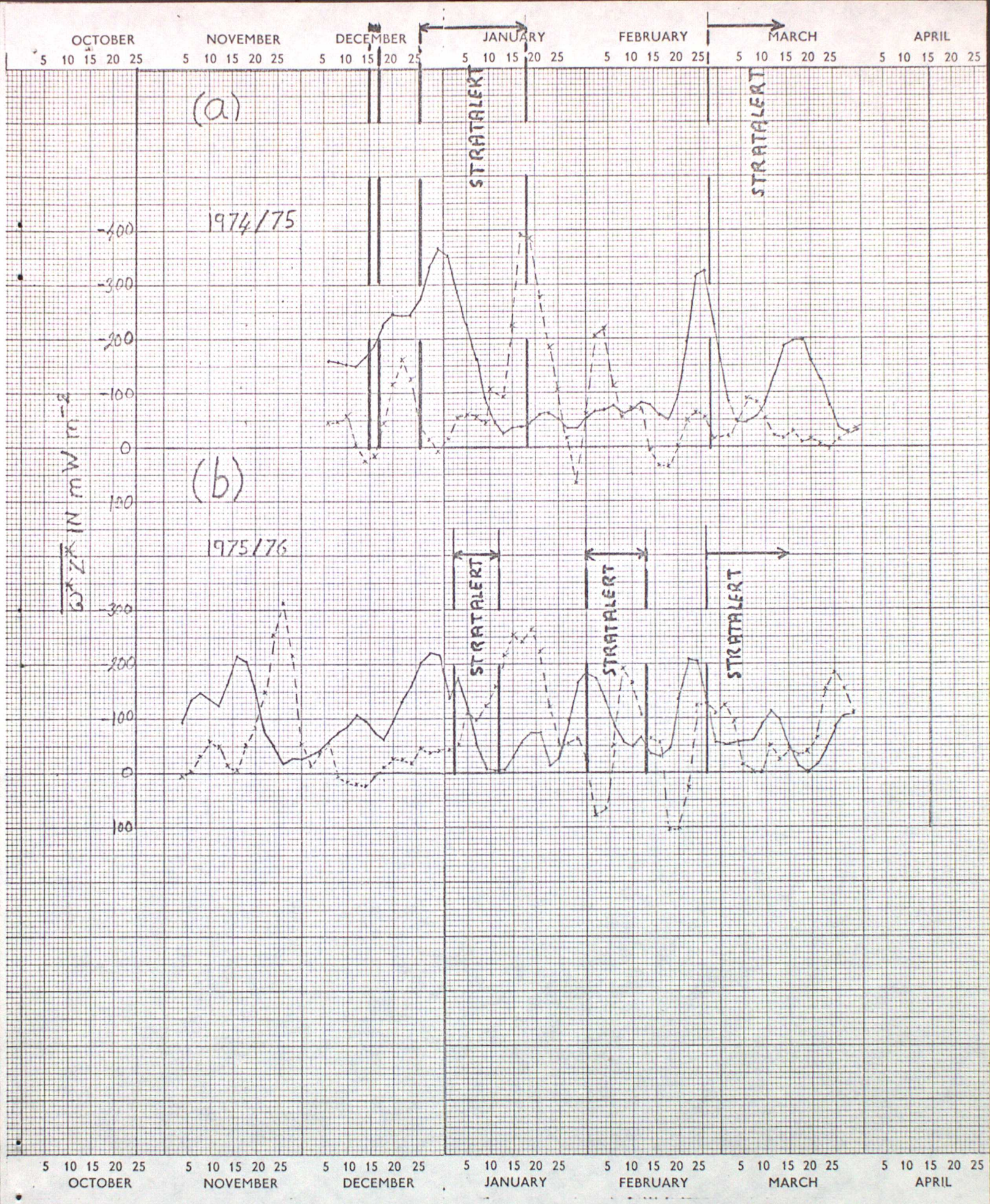

Figure 5. 100 mb flux of geopotential in wave numbers 1 and 2 for two winters (negative values indicate upward fluxes).

———— $\overline{W^* Z^*}$ (1)

x- - - -x $\overline{W^* Z^*}$ (2)

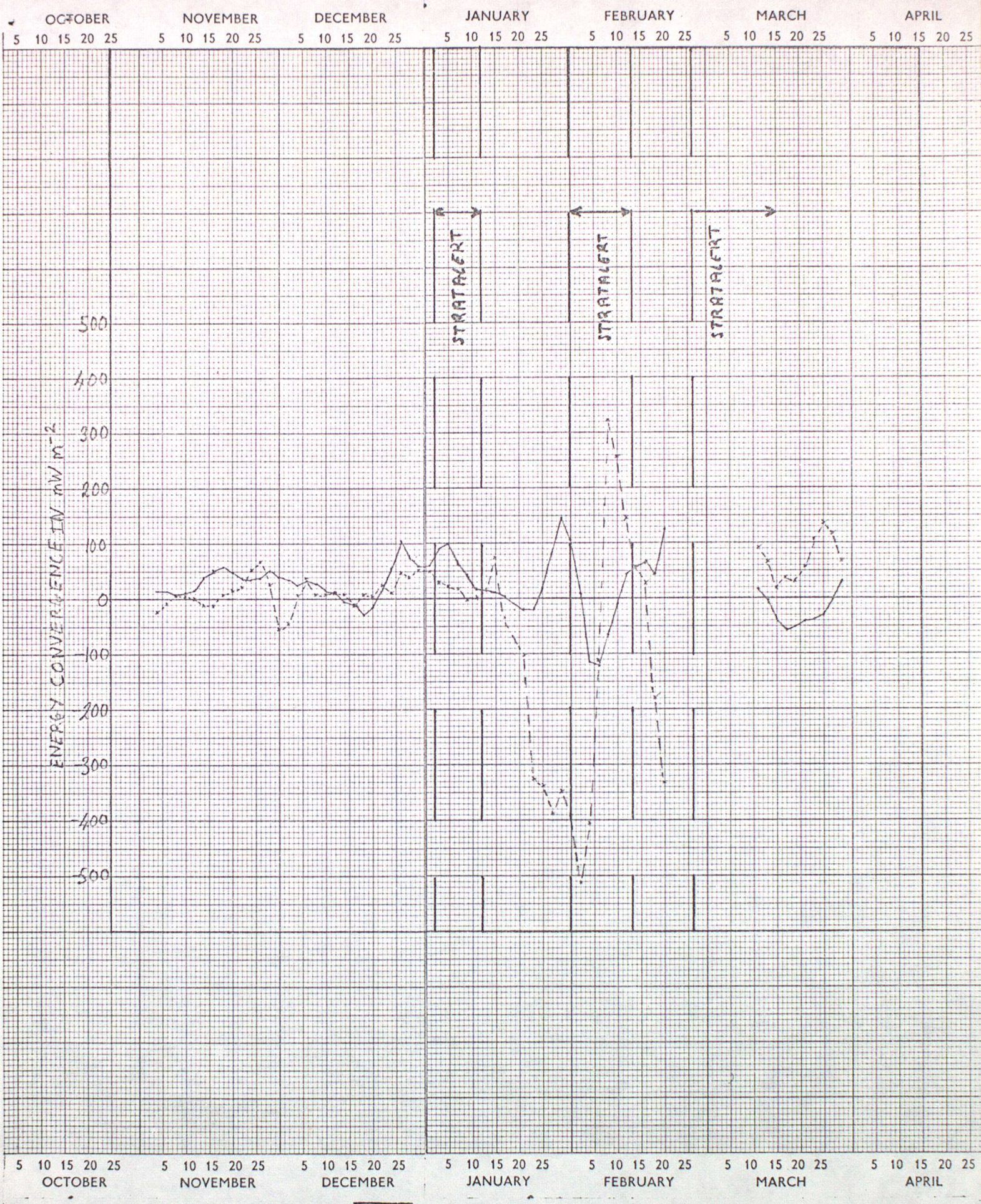

Figure 6. Convergence of $\overline{W^* Z^*}$ in wave numbers 1 and 2 in the 50 to 20 mb layer for 1975/76.

_____ wave number 1

x- - - -x wave number 2